

Calcium dependence of aequorin bioluminescence dissected by random mutagenesis

Ludovic Tricoire*, Keisuke Tsuzuki*, Olivier Courjean, Nathalie Gibelin, Gaëlle Bourout, Jean Rossier, and Bertrand Lambolez†

Laboratoire de Neurobiologie et Diversité Cellulaire, Centre National de la Recherche Scientifique, Unité Mixte de Recherche 7637, Ecole Supérieure de Physique et de Chimie Industrielles, 10 Rue Vauquelin, 75005 Paris, France

Communicated by J. Woodland Hastings, Harvard University, Cambridge, MA, April 20, 2006 (received for review October 12, 2005)

Aequorin bioluminescence is emitted as a rapidly decaying flash upon calcium binding. Random mutagenesis and functional screening were used to isolate aequorin mutants showing slow decay rate of luminescence. Calcium sensitivity curves were shifted in all mutants, and an intrinsic link between calcium sensitivity and decay rate was suggested by the position of all mutations in or near EF-hand calcium-binding sites. From these results, a low calcium affinity was assigned to the N-terminal EF hand and a high affinity to the C-terminal EF-hand pair. In WT aequorin, the increase of the decay rate with calcium occurred at constant total photon yield and thus determined a corresponding increase of light intensity. Increase of the decay rate was underlain by variations of a fast and a slow component and required the contribution of all three EF hands. Conversely, analyses of double EF-hand mutants suggested that single EF hands are sufficient to trigger luminescence at a slow rate. Finally, a model postulating that proportions of a fast and a slow light-emitting state depend on calcium concentration adequately described the calcium dependence of aequorin bioluminescence. Our results suggest that variations of luminescence kinetics, which depend on three EF hands endowed with different calcium affinities, critically determine the amplitude of aequorin responses to biological calcium signals.

EF hand | kinetics | luminescence | photoprotein | transduction

The photoprotein aequorin is a stable luciferase intermediate formed from the reaction of the protein apoaequorin (luciferase) and the substrate coelenterazine (luciferin), which emits light upon Ca^{2+} binding (1–5). Aequorin contains three EF-hand Ca^{2+} -binding sites (6–8) located close to its N (EF1) or C terminus (EF2,3 pair). Aequorin mutagenesis and crystal structure suggest that these three EF hands indeed bind Ca^{2+} , but their individual contribution to luminescence is still a matter of debate (9–13).

The steep increase of luminescence intensity with $[\text{Ca}^{2+}]$ makes aequorin a useful reporter of intracellular calcium signals (14). The formation of aequorin is a slow process (2), whereas the luminescence reaction is very fast and proceeds to completion in the continuous presence of Ca^{2+} . The aequorin response thus occurs as a flash that decays exponentially and whose onset rate does not depend on $[\text{Ca}^{2+}]$ (15). It has been observed early that the decay rate of this response increases with $[\text{Ca}^{2+}]$, whereas the total light emitted (light integral) remains relatively constant (15). This suggests that the increase of luminescence intensity with $[\text{Ca}^{2+}]$ is determined by variations of the decay rate but not of the light integral. In other words, the shorter the duration of the flash (i.e., the faster the decay), the larger the amplitude of the response (i.e., light intensity). However, the relationships among the intensity, the decay rate, and the integral of bioluminescence and their links to EF-hand occupancy have not been clearly established.

To analyze the contribution of decay kinetics to aequorin responses, we recently isolated aequorin mutants exhibiting slow decay rates (SloDK mutants) through random mutagenesis and functional screening (16). This procedure allows the selection of mutants that most efficiently affect a specific subfunction of a

protein with minimal alteration of its overall structure–function relationships. A different screening process yielded other mutants (Bright) exhibiting high luminescence in bacteria because of increased Ca^{2+} sensitivity or photoprotein stability (16). In contrast to SloDK mutants in which both Ca^{2+} sensitivity and decay rate are modified, Bright mutants show modifications of Ca^{2+} sensitivity with little change of decay rate. Both SloDK and Bright mutants carried single amino acid substitutions located in EF hands or their adjacent α -helices. Here, the dependence of mutant and WT aequorin luminescence on $[\text{Ca}^{2+}]$ was analyzed and combined with modeling to examine the contribution of the three EF hands and the role of decay kinetics in aequorin responses. We found that EF hands have different Ca^{2+} affinities, and all contribute to the variations of decay rate that determine the increase of luminescence intensity with $[\text{Ca}^{2+}]$.

Results

Bright and SloDK mutations (16) affect residues conserved in other photoproteins (see the supporting information, which is published on the PNAS web site), located either in EF hands at canonical Ca^{2+} -binding positions (8) or in their adjacent α -helices (Fig. 1A). Each SloDK mutation was selected several times independently during the screening of random mutants (16), and four of them similarly consisted in a D/E to G substitution at an EF-hand border. This observation suggests that SloDK mutations efficiently affect the decay rate, whereas other aequorin properties remain relatively unaffected. Indeed, the luminescence decay rates of SloDK mutants were strikingly slow, with half-decay times ranging from 20- (F^{149}S) to 57-fold (E^{35}G) greater than that of WT aequorin (Fig. 1B). In contrast, luminescence half-decay times of Bright mutants were similar to or only slightly slower than WT.

Luminescence Intensity. The $[\text{Ca}^{2+}]$ dependence of luminescence intensity was examined first. Because in our experimental setup, recording started after the peak of bioluminescence (see *Materials and Methods*), curves were plotted from initial maximum intensity measured upon Ca^{2+} addition (Fig. 2A). The plot of the L^{170}I mutant, very close to that of Q^{168}R , was omitted for clarity. EC_{50} s for Ca^{2+} interpolated from these curves (Fig. 1B) are used as an index of Ca^{2+} sensitivity.

The three mutants of the EF1 region showed a higher sensitivity to Ca^{2+} than WT aequorin. The effect of N^{26}D likely results from an increased EF1 affinity, consistent with the replacement of the polar Ca^{2+} -binding asparagine residue by a negatively charged residue. The effect of E^{35}G seems paradoxical, given that this mutation removes an essential Ca^{2+} -binding side chain (8, 17). This can be resolved by assuming that EF1 has lower Ca^{2+} affinity than EF2 and EF3, and that E^{35}G impairs

Conflict of interest statement: No conflicts declared.

*L.T. and K.T. contributed equally to this work.

†To whom correspondence should be addressed. E-mail: bertrand.lambolez@snv.jussieu.fr.

© 2006 by The National Academy of Sciences of the USA

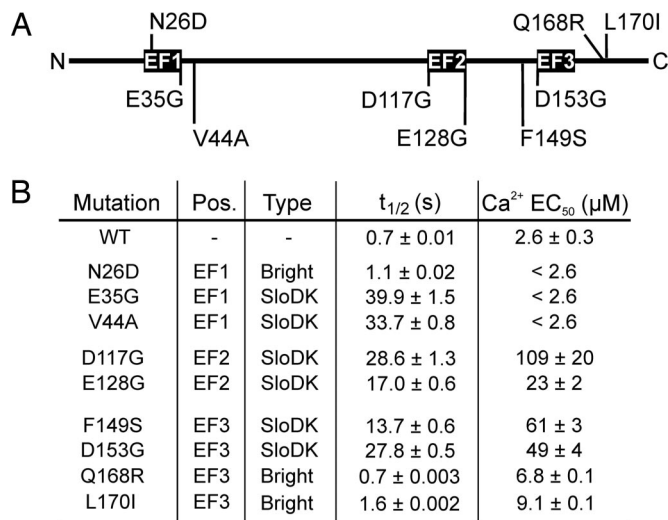


Fig. 1. Bright and SloDK aequorin mutants. (A) Bright (top) and SloDK (bottom) mutations of apoaequorin were located inside EF hands (■) or nearby. (B) Times to reach half of initial light ($t_{1/2}$) obtained at saturating $[Ca^{2+}]$ for WT and mutant aequorins reflect luminescence decay kinetics. Ca^{2+} EC_{50} values were derived from curves of $[Ca^{2+}]$ -dependent luminescence intensities.

EF1 contribution to the response to Ca^{2+} . Similarly, $V^{44}A$ may also impair contribution of EF1 to bioluminescence, thus increasing the relative contribution of the high affinity EF2 and EF3. Indeed, V^{44} interacts with the A^{40} coelenterazine-binding residue (11).

Mutants of the EF2 and EF3 domains exhibited a lower Ca^{2+} sensitivity than WT aequorin. The effects of $D^{117}G$, $E^{128}G$, and $D^{153}G$ are consistent with inactivation of either of the high-affinity EF2 or EF3 because of removal of an essential Ca^{2+} -binding side chain. The effect of $F^{149}S$, which suppresses a bond that links EF3 to the W^{129} coelenterazine-binding residue (16), presumably results from impairment of EF3 contribution to bioluminescence. The effect of $Q^{168}R$ likely results from interactions of arginine with several Ca^{2+} binding residues of EF3 (16).

These results are consistent with EF1 having a lower affinity to Ca^{2+} than EF2 and EF3. Analyses of double EF-hand mutants combining $E^{35}G$, $E^{128}G$, and $D^{153}G$ substitutions (Fig. 2B) confirmed the differences in EF-hand Ca^{2+} affinities and indicate that a single EF hand is sufficient to trigger bioluminescence. For these mutants, where only one EF hand was left intact, Ca^{2+} EC_{50} values were $34 \pm 9 \mu$ M for $EF1^{-2^{-}3^{-}}$, $6.1 \pm 0.1 \mu$ M for $EF1^{-2^{+}3^{-}}$, and $7.6 \pm 0.6 \mu$ M for $EF1^{-2^{-}3^{+}}$. The Ca^{2+} sensitivities of $EF1^{-2^{+}3^{-}}$ or $EF1^{-2^{-}3^{+}}$, lower than that of WT, suggest that mutation of either EF hand of the EF2,3 pair reduced the affinity of the remaining EF hand, as reported for other Ca^{2+} -binding proteins (8, 17). Hence, affinities of WT EF2 and EF3 are presumably higher than suggested by the Ca^{2+} sensitivities of $EF1^{-2^{+}3^{-}}$ or $EF1^{-2^{-}3^{+}}$ mutants.

These results indicate that the three EF hands are endowed with different Ca^{2+} affinities, and all contribute to the sensitivity of WT aequorin to $[Ca^{2+}]$.

Luminescence Decay Kinetics and Light Integral. Luminescence decays were next analyzed to examine the relationships of the decay rate and light integral with the intensity of the response to Ca^{2+} (Fig. 3). Decays of WT and mutant aequorins were best fitted with two exponentials (see supporting information). Time constants of these fast and slow exponentials (τ_F and τ_S , respectively) and their light integrals (Σ_F and Σ_S , respectively) were determined and plotted together with total light integral ($\Sigma_T = \Sigma_F + \Sigma_S$) and initial

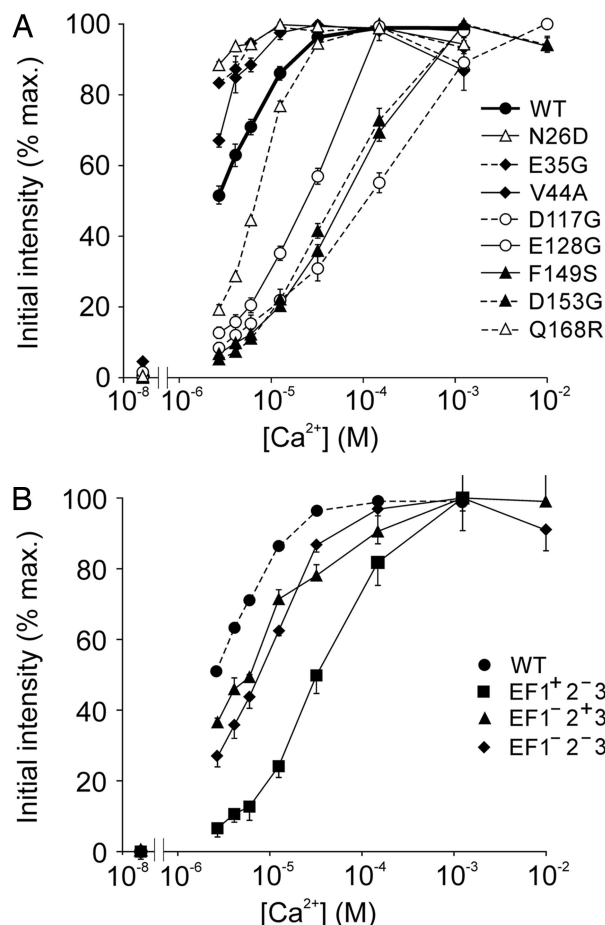


Fig. 2. Initial maximum intensity against $[Ca^{2+}]$ of mutant and WT aequorins. (A) Bright and SloDK mutants. The plot of the $L^{170}I$ Bright mutant (not shown) was almost identical to that of $Q^{168}R$. (B) Double EF-hand mutants. $EF1^{-2^{-}3^{-}}$, $EF1^{-2^{+}3^{-}}$, and $EF1^{-2^{-}3^{+}}$ correspond to the $E^{128}G$ and $D^{153}G$, $E^{35}G$ and $D^{153}G$, and $E^{35}G$ and $D^{128}G$ double mutants, respectively.

maximum intensity. Because kinetics of SloDK mutants for a given EF hand (e.g., $E^{35}G$ and $V^{44}A$ for EF1) were similar, only one example is displayed per EF hand. Kinetics of $Q^{168}R$ and $L^{170}I$ Bright mutants (not shown) were similar to WT, except for a shift toward higher $[Ca^{2+}]$. Similar results were obtained on WT aequorin and the $D^{153}G$ mutant by using a fast-mixing stopped-flow apparatus (see supporting information).

For WT aequorin, the decay rate increased with $[Ca^{2+}]$ (Fig. 3 Top), whereas Σ_T was maximal at low $[Ca^{2+}]$ and remained roughly constant (Fig. 3 Bottom). Indeed, correction for the lag preceding the activity measurement (see Materials and Methods and supporting information) yielded a Σ_T value at 1.24 mM Ca^{2+} , which was decreased to only 91.5% of maximum. Variations of the decay rate thus determined the increase of initial intensity. The curves of initial intensity and Σ_F were almost superimposed, indicating that variations of τ_S contributed little to the increase of the decay rate. Hence, the increase of luminescence intensity was driven primarily by the Σ_F/Σ_T ratio (not shown), which increased from $25.5 \pm 2.2\%$ at 2.7μ M Ca^{2+} to $51.2 \pm 0.4\%$ at 1.24 mM Ca^{2+} .

$N^{26}D$ essentially differed from WT in that Σ_F decreased with increasing $[Ca^{2+}]$, whereas Σ_S remained roughly constant. As a consequence, $N^{26}D$ exhibited a much smaller increase of decay rate and thus of initial intensity than WT. In contrast with WT and Bright mutants, the luminescence decay rates of SloDK mutants decreased with increasing $[Ca^{2+}]$. These mutants ex-

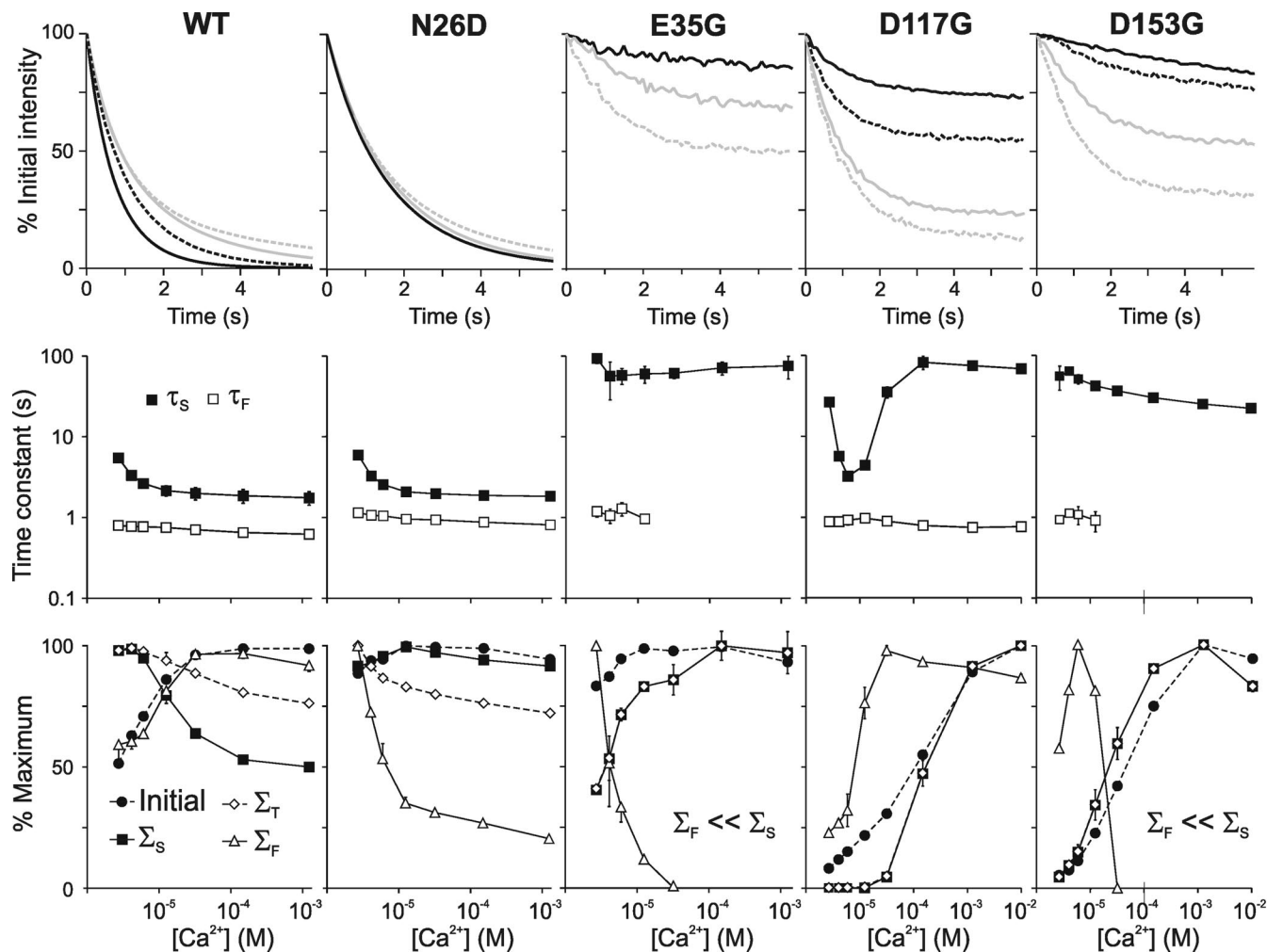


Fig. 3. Decay kinetics of WT aequorin and EF-hand mutants. (*Top*) Unitary recordings show variations of decay kinetics between low (dotted gray), medium low (gray), medium high (dotted black), and high (black) $[Ca^{2+}]$. (*Middle*) Plots of the time constants of fast (τ_F) and slow (τ_S) exponentials vs. $[Ca^{2+}]$ (x axis as in *Bottom*). In $E^{35}G$ and $D^{153}G$, τ_F values could not be determined above $12.5 \mu M$ Ca^{2+} because of breakdown of S_F . (*Bottom*) Light integrals of the fast (Σ_F) and slow (Σ_S) exponentials and of total light emitted ($\Sigma_T = \Sigma_F + \Sigma_S$) vs. $[Ca^{2+}]$. Initial intensities are plotted for comparison.

hibited high τ_S and Σ_S/Σ_T values and extensive variations of Σ_T , which determined to a large extent the increase of initial intensity.

The τ_F value varied little with $[Ca^{2+}]$ or between WT and mutants, suggesting it is an intrinsic constant of aequorin luminescence. In WT, τ_F was 615 ± 21 ms at 1.24 mM Ca^{2+} , close to the 833 ms reported assuming monoexponential decay (15). In contrast, other kinetic parameters appeared to depend on EF-hand domains. All SloDK mutations resulted in high τ_S and Σ_S/Σ_T values and altered their variations. Hence, these parameters did not rely on any single EF hand. Σ_F showed a critical dependence on both EF1 and EF3. Indeed, Σ_F/Σ_T was negligible in $E^{35}G$ and $D^{153}G$ (maximum, $1.1 \pm 0.4\%$ and $3.6 \pm 1.1\%$, respectively). $EF2^-$ SloDK mutants exhibited a markedly different behavior. In these latter mutants, Σ_F persisted throughout the whole $[Ca^{2+}]$ range (maximum, Σ_F/Σ_T ; $42.8 \pm 5.2\%$ at $12.5 \mu M$ Ca^{2+} for $D^{117}G$), whereas τ_S first decreased (in the range of EF3 affinity) and then increased (in the range of EF1 affinity) with increasing $[Ca^{2+}]$. This observation suggests a distinctive role for EF2, perhaps in the functional coupling between EF1 and EF3 domains.

Decays of double EF-hand mutants (not shown) analyzed at saturating $[Ca^{2+}]$ exhibited both a fast and a slow component, confirming these are intrinsic to aequorin luminescence. Values

of τ_F were 5.9 ± 0.1 s, 5.5 ± 0.3 s, and 8.4 ± 0.5 s and of τ_S were 122 ± 6 s, 275 ± 7 s, and 341 ± 28 s for $EF1^+2^-3^-$, $EF1^-2^+3^-$, and $EF1^-2^-3^+$ mutants, respectively. Decays of these mutants were governed by the slow component ($\Sigma_S/\Sigma_T > 98\%$).

The present data suggest that in WT aequorin, all EF hands contribute to the decay rate increase by modulating the Σ_F/Σ_T ratio, which in turn determines the increase of peak intensity at constant light integral.

Contribution of Q^{168} and L^{170} to Decay Kinetics. The QHL[168–170] residues interact with both the E^{164} Ca^{2+} -binding residue of EF3 and coelenterazine (via the E^{164} - Q^{168} and H^{169} -coelenterazine bonds; see ref. 11) and may help trigger bioluminescence (16). These interactions provide a rationale for the lower Ca^{2+} sensitivity of $Q^{168}R$ and $L^{170}I$ mutants and suggests these residues contribute to decay kinetics. Indeed, screening of a library of random Q^{168} and L^{170} mutants resulted in the isolation of mutants exhibiting a large range of decay rates (see supporting information). Among selected clones, the $Q^{168}A$ and $L^{170}V$ mutant (designated AHV) and the mutant combining $Q^{168}R$ and $L^{170}I$ Bright mutations (designated RHI) were characterized in detail. Indeed, their Ca^{2+} sensitivities were reduced to a similar extent (EC_{50} values: 28 ± 2 and $16.5 \pm 0.6 \mu M$ for AHV and RHI, respectively), but their decay rates differed markedly (Fig. 4).

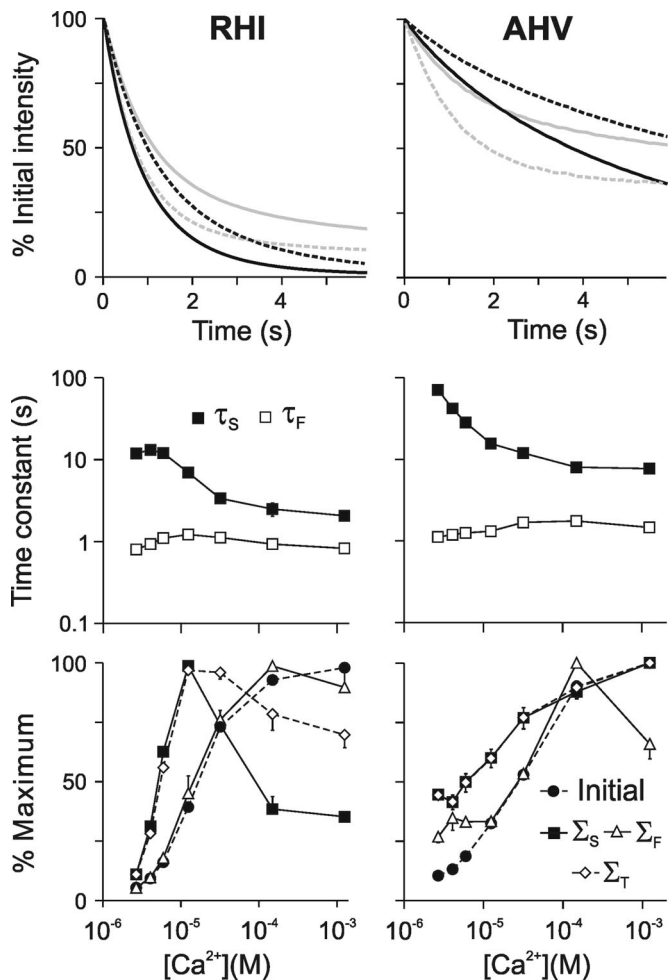


Fig. 4. Decay kinetics of Q¹⁶⁸ and L¹⁷⁰ double mutants. RHI, Q¹⁶⁸R and L¹⁷⁰I; AHV, Q¹⁶⁸A and L¹⁷⁰V. (Top) Unitary recordings show decay kinetics at low (dotted gray line), medium low (gray line), medium high (dotted black line), and high (black line) [Ca²⁺]. (Middle) Time constants of fast (τ_F) and slow (τ_S) exponentials vs. [Ca²⁺] (x axis as in Bottom). (Bottom) Light integrals of the fast (Σ_F) and slow (Σ_S) exponentials, of total light emitted ($\Sigma_T = \Sigma_F + \Sigma_S$), and of initial intensity vs. [Ca²⁺].

RHI bioluminescence exhibited all of the key features of WT but shifted toward higher [Ca²⁺]. This shift allowed the initial increases of Σ_F , Σ_S , and Σ_T , which occurred below 2.7 μ M Ca²⁺ for WT, to be observed above this concentration for RHI. In this initial phase, Σ_S and Σ_T increased in parallel and reached a maximum at 12.5 μ M Ca²⁺. Beyond this point, Σ_T remained close to its maximum (corrected Σ_T for lag between injection and measurement, 84.2% at 1.24 mM Ca²⁺), whereas kinetics varied extensively. As for WT, most of the increase of RHI initial intensity with [Ca²⁺] resulted from an increase of Σ_F . Hence, RHI mutations reduced EF3 Ca²⁺ affinity but left the transduction of Ca²⁺ induced conformational changes to bioluminescence unaffected.

In contrast, the slow decay kinetics of AHV suggests that the contribution of EF3 to the response to Ca²⁺ was reduced in this mutant. Indeed, AHV kinetics exhibited high τ_S and Σ_S/Σ_T values and Σ_T variations extending over a large [Ca²⁺] range, as found in EF3⁻ SloDK mutants. This presumably resulted in part from the disruption of the E¹⁶⁴-Q¹⁶⁸ interaction. However, the decrease of τ_S and the persistence of Σ_F throughout the whole [Ca²⁺] range (Σ_F/Σ_T , 2.5 \pm 0.7% at 1.24 mM Ca²⁺) suggest that, in contrast with EF3⁻ SloDK mutants, the participation of EF3 to bioluminescence was not abolished in the AHV mutant.

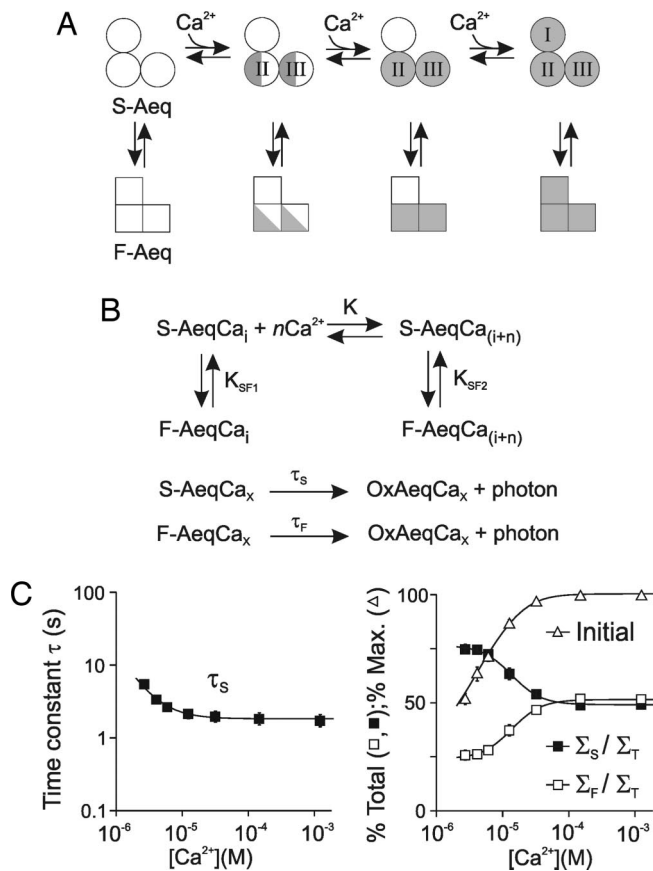


Fig. 5. A model of WT aequorin Ca²⁺ dependence. (A) Ca²⁺-binding pathways and interconversion between a slow (S) and a fast (F) light-emitting state. Ca²⁺-bound EF hands are shown in gray. (B Upper) Interconversion equilibria describing evolution of S and F state proportions with Ca²⁺ binding. (B Lower) Kinetics of light emission from Ca²⁺-bound S and F states. (C) Comparison of experimental values of kinetic parameters (symbols) with the best fit of the model (curves).

These data confirm that slow decay kinetics result from the disruption of a link between a given EF-hand domain and coelenterazine-binding residues but not from the reduction of its calcium affinity.

A Model of Aequorin Ca²⁺ Dependence. The present results suggest that the three EF hands contribute to luminescence, and that varying proportions of a slow and a fast light-emitting state (S-Aeq and F-Aeq, respectively) determine the increase of the decay rate and thus of light intensity. These findings are summarized in Fig. 5A, which postulates that EF1 has lower Ca²⁺ affinity than EF2 and EF3. This scheme does not infer sequential Ca²⁺ binding to the different EF hands but describes their occupancy with increasing [Ca²⁺].

None of the reaction schemes and models of aequorin luminescence proposed so far (15, 18) takes into account the variations of decay rate with [Ca²⁺] as a key determinant of light intensity. Hence, we investigated whether a model based on these variations may capture the essential features of aequorin responses to Ca²⁺ (Fig. 5B; see equations in supporting information). This model postulates (i) an equilibrium between S-Aeq and F-Aeq whose interconversion constant (K_{SF}) depends on the number of Ca²⁺ bound; (ii) Σ_F/Σ_T and Σ_S/Σ_T vary with the binding of n Ca²⁺ to an initial Ca²⁺-bound specie (S-AeqCa_{*n*}); (iii) τ_F is independent of [Ca²⁺] (set at mean experimental value), and τ_S varies with the binding of Ca²⁺ to m sites; and (iv)

light-emission efficiency Σ_T ($\Sigma_F + \Sigma_S$) is constant for all Ca^{2+} -bound species.

Parameters of the equation describing theoretical τ_S were optimized to fit experimental τ_S values measured for WT aequorin (see supporting information). The best fit (see curve in Fig. 5C) was obtained with $m = 1.5 \text{ Ca}^{2+}$, binding with an apparent dissociation constant of $3.8 \mu\text{M}$. Hence, acceleration of τ_S in WT aequorin requires binding of more than one Ca^{2+} in our model. Similar optimization was performed for theoretical Σ_S/Σ_T . The best fit (see Σ_S/Σ_T and Σ_F/Σ_T curves in Fig. 5C) was obtained with $K_{SF1} = 0.3$, $K_{SF2} = 1$, and $n = 1.9 \text{ Ca}^{2+}$ binding with an apparent dissociation constant of $17 \mu\text{M}$. These values imply that in our model, the proportion of molecules in the F state increases (because of $K_{SF2} > K_{SF1}$) as a result of the binding of more than one Ca^{2+} . Because aequorin contains only three EF hands, the m and n values derived from the best fit predict that at least one EF hand is involved in both τ_S and Σ_F/Σ_T variations, consistent with their overlapping $[\text{Ca}^{2+}]$ ranges. Our model predicts that SloDK mutations have a major effect on K_{SF} interconversion constants. Although EF1^- and EF3^- mutations would decrease both K_{SF1} and K_{SF2} , EF2^- mutations would leave K_{SF1} relatively unaffected.

Finally, evolution of the theoretical initial intensity with $[\text{Ca}^{2+}]$ was calculated from Σ_S/Σ_T , Σ_F/Σ_T , and τ_S values derived from the best fit, with constant τ_F (see supporting information). The good match observed between theoretical and experimental values (Fig. 5C Right) indicates that the present model of WT aequorin adequately describes the parallel increases of light intensity and decay rate with $[\text{Ca}^{2+}]$ occurring at constant light integral.

Discussion

The contribution of aequorin EF-hand domains to bioluminescence was dissected by using mutants of decay kinetics and Ca^{2+} sensitivity. All EF-hand domains contributed to Ca^{2+} sensitivity, with EF1 showing lower affinity than EF2 and EF3, and each individual EF hand was able to trigger luminescence. Decay kinetics of WT aequorin consisted of a slow and a fast component whose variations determined those of luminescence intensity in a large $[\text{Ca}^{2+}]$ range where the light integral was constant. All EF-hand domains contributed to these variations. These findings were used to design a model that adequately described the Ca^{2+} dependence of WT aequorin.

SloDK Mutations Impair Transduction of Ca^{2+} Binding to Bioluminescence. In EF-hand-based Ca^{2+} sensors like aequorin and calmodulin, Ca^{2+} binding induces conformational changes that trigger activity (8). Although Bright mutations essentially shifted Ca^{2+} sensitivity curves, SloDK ones additionally decreased the rate of light emission, presumably by disrupting a structural link that allows a given EF hand to trigger luminescence. Indeed, D/E to G substitutions at EF1–EF3 extremities likely uncouple the EF hand from the protein scaffold by increasing the flexibility of its joint to the adjacent α -helix. The V^{44}A and F^{149}S mutations do not affect Ca^{2+} -binding residues and may thus specifically impair conformational changes. Such a case has been reported for calmodulin, where the EF3-neighboring mutation F^{92}A impairs conformational changes without reducing Ca^{2+} affinity (19). The F^{149}S mutation suppresses a link of EF3 to the W^{129} coelenterazine-binding residue (16). Moreover, the V^{44}A mutation may affect the interaction of V^{44} with the A^{40} coelenterazine-binding residue (11). Interestingly, corresponding residues of the photoprotein obelin both interact with coelenterazine (A^{46} and I^{50} ; see supporting information and ref. 20). Finally, RHI and AHV mutants provide an example of mutations at the same positions that resulted in similar Ca^{2+} EC₅₀s but very different decay rates. Part of this difference can be attributed to disruption of the E^{164} – Q^{168} bond that links EF3 conformational

changes to bioluminescence (16). It thus appears that SloDK mutants all disrupt a structural link that allows Ca^{2+} binding to trigger bioluminescence.

Functional Domains of Aequorin. The structures of photoproteins suggest that each of the three EF-hand domains forms a functional unit (11, 20). Indeed, results with double EF-hand mutants indicate that each individual EF hand is able to trigger aequorin bioluminescence. Nonetheless, distinctive functional properties could be assigned to each of the three EF-hand domains, based on the different effects of their respective mutations. These differences appear very significant, given the high similarity between the effects of the two SloDK mutations found for each EF hand. Our results define a low Ca^{2+} affinity EF1 domain and a high-affinity domain comprising the EF2,3 pair, consistent with a previous report showing that aequorin binds two Ca^{2+} with a high affinity and an additional Ca^{2+} with 22 times lower affinity (21). The N- and C-terminal domains of calmodulin similarly exhibit low and high Ca^{2+} affinity, respectively (17). Interestingly, the cooperativity between aequorin EF2,3 for Ca^{2+} binding, suggested by the low affinity of $\text{EF1}^-2^+3^-$ or $\text{EF1}^-2^-3^+$ mutants as compared to WT, is also observed for the C-terminal EF-hand pair of calmodulin (17). Finally, $[\text{Ca}^{2+}]$ dependence of kinetic properties relied heavily on EF1 and EF3 but less on EF2 (see Σ_F and τ_S in EF2^- mutants), which may be preferentially involved in the coupling between the low-affinity EF1 and the high-affinity EF3. Previous studies reported that aequorin bioluminescence involves the binding of two or more Ca^{2+} (18, 21). Our results indicate that, although each individual EF hand is sufficient to trigger luminescence, all three EF hands participate in the dependence of WT aequorin luminescence on $[\text{Ca}^{2+}]$.

Decay Kinetics, Light Integral, and Initial Maximum Intensity. Our data show that in WT aequorin, both the light intensity and the decay rate are greater at higher $[\text{Ca}^{2+}]$, such that the total light (integral, Σ_T) is the same at different Ca^{2+} concentrations. Although the $[\text{Ca}^{2+}]$ dependence of the decay rate has been reported early (15), the present study reveals that it results from variations of a fast and a slow component. The fast and slow components coexisted across mutants and Ca^{2+} concentrations and were even observed in double EF-hand mutants where only one EF hand is left unaffected. Our results thus suggest that the slow and fast light-emitting states coexist, and that their proportions evolve concomitantly, rather than sequentially along a single linear pathway. In any sequential model, τ_F and τ_S would evolve in the same $[\text{Ca}^{2+}]$ range as Σ_F/Σ_T and Σ_S/Σ_T , which is in contradiction with our observations. In contrast, our parallel model allows dissociating variations of the different kinetic parameters and adequately describes variations of light intensity with $[\text{Ca}^{2+}]$.

A key feature of WT aequorin is that Σ_T reached a maximum at low $[\text{Ca}^{2+}]$ and remained roughly constant in a wide $[\text{Ca}^{2+}]$ range where major variations of decay kinetics occurred. Given the existence of only three EF hands in aequorin (6, 7, 13), this observation suggests that Σ_T variations rely primarily on the binding of only one Ca^{2+} , as postulated in the present model, whereas the three EF hands are involved in variations of decay rate and thus of peak intensity. It is likely that the light-emission rate resulting from single EF-hand occupancy is higher in WT aequorin, where the rigidity of the photoprotein scaffold is unaffected, than in double EF-hand mutants.

Aequorin Luminescence as a Biological Signal. The fast kinetics of photoprotein luminescence provides a sensitive means of studying the early steps, which lead from calcium binding to activation of EF-hand-based calcium sensors. The structural homology among various photoproteins suggests that their $[\text{Ca}^{2+}]$ depen-

dence obeys the same rules, despite different maximum luminescence rates (22, 23). Photoproteins contain a pseudo-EF-hand motif, which does not bind Ca^{2+} (6, 13). Its position relative to the three EF hands in the primary sequence, which defines a pattern similar to the two EF-hand pairs of calmodulin, has suggested that photoproteins have evolved from a calmodulin ancestor gene toward bioluminescence (24). As underlined above, some of the present findings may apply to calmodulin and other Ca^{2+} sensors that rely on several EF hands exhibiting different affinities to transduce Ca^{2+} stimuli into biological signals.

Aequorin occurs in the jellyfish *Aequorea*, where it forms a readily mobilizable source of light used to generate a rapid luminescent signal in response to Ca^{2+} transients. In contrast with typical enzymatic systems where the substrate is metabolized only upon activation, aequorin is a reaction intermediate where the coelenterazine substrate is already consumed. Our results indicate that the Ca^{2+} dependence of aequorin luminescence relies on variations of the light emission rate occurring at constant maximal photon yield. Variations of the light-emission rate allow the intensity of the light signal to reflect the amplitude of Ca^{2+} transients. It is noteworthy that the steadiness of the photon yield allows aequorin consumption to be proportional to the amplitude of a transient light signal. If, alternatively, variations of the photon yield were responsible for variations of light intensity, this would imply nonradiative energy dissipation in case of submaximal luminescence response. The mechanisms of aequorin Ca^{2+} dependence thus appear well adapted to the function of the signal emitter in the jellyfish, which depends on its diet as an exclusive source of coelenterazine (25).

Materials and Methods

Cell-free expression of WT and mutant apoproteins was performed as described (16) by using the Rapid Translation System (RTS, Roche Diagnostics, Mannheim, Germany) from cDNAs subcloned in the pRSETc expression vector (Invitrogen). Reactions were diluted 1:1 in glycerol, and this working stock was stored at -20°C .

Aequorin was reconstituted for 1 h at 4°C in the presence of 10 mM 1,4-DTT/50 mM Tris (pH 8)/10 μM EDTA/5 μM

coelenterazine, and then diluted 20 times into 50 mM Tris (pH 8)/10 μM EDTA to minimize the coelenterazine luminescence background. Fifty microliters of this solution (corresponding to 0.2 μl of apoaequorin working stock) was used per well for luminescence assay performed in 96-well plates. Aequorin activity was measured at 22°C in a PhL microplate luminometer (Mediator, Vienna) by injecting 100 μl of solutions containing 50 mM Tris (pH 8) with variable CaCl_2 concentrations buffered with 10 μM EDTA. The free $[\text{Ca}^{2+}]$ immediately after mixing were calculated from affinity constants of EDTA by using the WEBMAXC, Ver. 2.22, program (www.stanford.edu/~cpatton/webmaxcSR.htm; see ref. 26), taking into account 3 μM contaminating Ca^{2+} . Indeed, contaminating $[\text{Ca}^{2+}]$ found in a 50 mM Tris (pH 8) solution was 3.5 μM , as determined by elemental analysis or 3 μM free Ca^{2+} , measured by fluorescence of the Calcium Green indicator calibrated against the Calcium Calibration Buffer kit (Molecular Probes).

Data were collected with 0.1-s integration time. Luminescence exponential decays were analyzed by using the CLAMPFIT 8.1 software (Axon Instruments, Foster City, CA). Fast and slow components of double exponentials are described by their time constants (τ_F and τ_S , respectively) and their light integrals (Σ_F and Σ_S , respectively), whereas Σ_T represents the total light integral ($\Sigma_F + \Sigma_S$). In our PhL luminometer, injection of 100 μl solution required 280 ms, and recording started 365 ms after the beginning of the injection during the decay phase after luminescence onset (≈ 10 ms; see ref. 15). Corrected Σ_T values that appear in the text take into account this 365-ms lag and were calculated from the formula:

$$\Sigma_T = \Sigma_S e^{\frac{0.365}{\tau_S}} + \Sigma_F e^{\frac{0.365}{\tau_F}}$$

Each value represents the mean of at least two experiments performed in triplicate. Results are expressed as mean \pm SEM.

We thank J. Woodland Hastings, Alain-François Chaffotte, and Stephen Rees for their valuable help. This work was supported by Centre National de la Recherche Scientifique, Fondation pour la Recherche Médicale, and Novartis. L.T. was recipient of a Fondation pour la Recherche Médicale fellowship.

- Shimomura, O., Johnson, F. H. & Saiga, Y. (1962) *J. Cell. Comp. Physiol.* **59**, 223–239.
- Shimomura, O. & Johnson, F. H. (1975) *Nature* **256**, 236–238.
- Shimomura, O. & Johnson, F. H. (1978) *Proc. Natl. Acad. Sci. USA* **75**, 2611–2615.
- Hastings, J. W. & Gibson, Q. H. (1963) *J. Biol. Chem.* **238**, 2537–2554.
- Wilson, T. & Hastings, J. W. (1998) *Annu. Rev. Cell Dev. Biol.* **14**, 197–230.
- Inouye, S., Noguchi, M., Sakaki, Y., Takagi, Y., Miyata, T., Iwanaga, S., Miyata, T. & Tsuji, F. I. (1985) *Proc. Natl. Acad. Sci. USA* **82**, 3154–3158.
- Prasher, D., McCann, R. O. & Cormier, M. J. (1985) *Biochem. Biophys. Res. Commun.* **126**, 1259–1268.
- Lewit-Bentley, A. & Rety, S. (2000) *Curr. Opin. Struct. Biol.* **10**, 637–643.
- Tsuji, F. I., Inouye, S., Goto, T. & Sakaki, Y. (1986) *Proc. Natl. Acad. Sci. USA* **83**, 8107–8111.
- Kendall, J. M., Sala-Newby, G., Ghalaut, V., Dormer, R. L. & Campbell, A. K. (1992) *Biochem. Biophys. Res. Commun.* **187**, 1091–1097.
- Head, J. F., Inouye, S., Teranishi, K. & Shimomura, O. (2000) *Nature* **405**, 372–376.
- Toma, S., Chong, K. T., Nakagawa, A., Teranishi, K., Inouye, S. & Shimomura, O. (2005) *Protein Sci.* **14**, 409–416.
- Deng, L., Vysotski, E. S., Markova, S. V., Liu, Z. J., Lee, J., Rose, J. & Wang, B. C. (2005) *Protein Sci.* **14**, 663–675.
- Brini, M., Pinton, P., Pozzan, T. & Rizzuto, R. (1999) *Microsc. Res. Tech.* **46**, 380–389.
- Hastings, J. W., Mitchell, G., Mattingly, P. H., Blinks, J. R. & Van Leeuwen, M. (1969) *Nature* **222**, 1047–1050.
- Tsuzuki, K., Tricoire, L., Courjean, O., Gibelin, N., Rossier, J. & Lambolez, B. (2005) *J. Biol. Chem.* **280**, 34324–34331.
- Maune, J. F., Klee, C. B. & Beckingham, K. (1992) *J. Biol. Chem.* **267**, 5286–5295.
- Allen, D. G., Blinks, J. R. & Prendergast, F. G. (1977) *Science* **195**, 996–998.
- Meyer, D. F., Mabuchi, Y. & Grabarek, Z. (1996) *J. Biol. Chem.* **271**, 11284–11290.
- Liu, Z. J., Vysotski, E. S., Chen, C. J., Rose, J. P., Lee, J. & Wang, B. C. (2000) *Protein Sci.* **9**, 2085–2093.
- Shimomura, O. (1995) *Biochem. Biophys. Res. Commun.* **211**, 359–363.
- Morin, J. G. & Hastings, J. W. (1971) *J. Cell Physiol.* **77**, 305–312.
- Markova, S. V., Vysotski, E. S., Blinks, J. R., Burakova, L. P., Wang, B. C. & Lee, J. (2002) *Biochemistry* **41**, 2227–2236.
- Tsuji, F. I., Ohmiya, Y., Fagan, T. F., Toh, H. & Inouye, S. (1995) *Photochem. Photobiol.* **62**, 657–661.
- Haddock, S. H., Rivers, T. J. & Robison, B. H. (2001) *Proc. Natl. Acad. Sci. USA* **98**, 11148–11151.
- Bers, D. M., Patton, C. W. & Nuccitelli, R. (1994) *Methods Cell Biol.* **40**, 3–29.